Sensitivity of Hypersonic Flow to Wall/Gas Interaction Models Using DSMC

F. C. Hurlbut*
University of California, Berkeley, California

Studies of flow over a flat plate by the method of direct simulation using Monte Carlo (DSMC) are described; particular emphasis is placed on the influence of the wall/gas interaction model. Effects of the commonly used diffuse/specular combinations are compared with those for the baseline model employing fully accommodated diffuse molecular scattering. Computations using the baseline model are also compared with those for the lobular scattering model prepared by Hurlbut and Sherman on the basis of suggestions by Nocilla (HSN). Profound alterations from baseline distributions of the velocity and density fields are observed for specular/diffuse combinations and for the HSN models and significant effects on temperature distributions are also observed.

Background

THE method of direct simulation by Monte Carlo (DSMC) makes possible the study of hypersonic flows for a broad range of Knudsen numbers characterizing the rarefied gas regimes. Its capability has been shown through recent applications to bodies of complex geometry in swift passage through dissociating and reacting atmospheres as discussed, for example, by Moss and Bird,[1] Moss,[2] or Cuda and Moss.[3] Confidence in the method's predictive value has been strengthened by the generally excellent agreement between DSMC results and those of other computational methods, as summarized in Ref. 4, and by comparison with wind tunnel results, as in Dahlen and Brundin[5] or Bird.[6] Such comparisons have not dealt with the details of experimental flowfields, except in rare instances (see Ref. 7), owing to the scarcity of such information. It should be remarked in this connection that for most low enthalpy flows over technical surfaces the diffuse scattering model for wall interactions seems quite adequate, although small departures from this model would appear to have been present in the flat plate flows studied by Becker et al.[8] that are discussed in this paper.

Impressive agreement has also been shown between DSMC and experimental heat-transfer results for the Shuttle Orbiter at 92.5 km.[1] However, at larger altitudes DSMC overpredicts the heat-transfer coefficient, as measured along the windward stagnation line, the DSMC coefficient at 110 km being ~ 2.7 times the experimental value. When the assumption is made that 50% of incident molecules are specularly scattered, the overprediction is reduced to a factor of about 1.5. It would seem from this predictive discrepancy, and, of course, from many other indications (see the author's review, Ref. 9) that we cannot expect the wall interaction to be represented correctly for bodies at orbital velocities by the model of fully thermally accommodated, diffuse scattering.

In developing understanding of what is clearly an exceedingly complex problem, it is useful to examine the sensitivity of rarefied gas flows over a surface to changes in the wall interaction model, and it is with that examination that this paper is primarily concerned. The method of DSMC introduced by Bird is used to model the flow of helium gas traversing a two-dimensional field. The "lower" boundary (the active surface) as shown in Fig. 1, is 54 cell lengths in extent along the axial direction x, preceded by a guard strip extending 6 cell lengths from the entry plane. The guard strip reflects incident molecules specularly, by which process the normal momentum of the particle is reversed while its momentum parallel to the surface is retained. There is provided, in effect, a region of freeflow immediately followed by an active surface having an ideally sharp leading edge. The "upper" bounding surface of the field also is specularly reflecting and is placed at a distance of 30 cell heights (y axis) above the active surface. Several of the cases were also run using 37 or 45 cell heights. The transverse extent of the field is immaterial, since the z coordinate of molecules is not used. However, a cell volume is specified, and for this purpose (a convenience in bookkeeping) a field "width" in the z direction is defined.

The Bird method is widely known and as it was used in the present calculations without substantive change except, of course, for the provision of code for gas/wall interactions, it will not be elaborated on here. The studies that I describe are small in scale in terms of required machine capability and were run comfortably on a modern personal computer. In all of the cases discussed, from 1800–2700 cells were used in the field, and an array space for 20,000–30,000 molecules was provided. Typically, 200,000–500,000 collisions were calculated during a run. Material calculated and printed out included the number of wall interactions on the active surface, the coordinate mean velocities in each cell, the translational temperatures, mass and number densities, the ratio of local density to entering freestream density, the mean free path, and the ratio of local free path to that of the freestream.

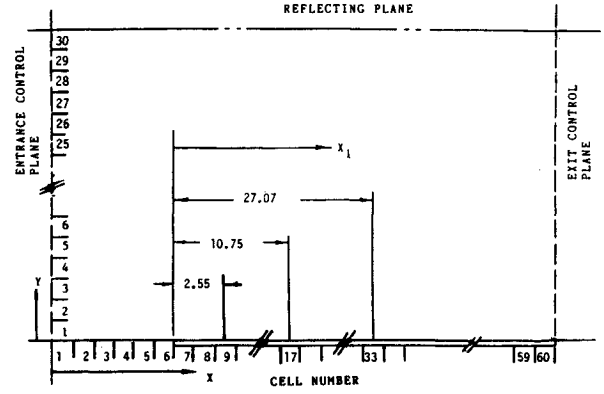

Fig. 1 Model flowfield geometry.

Presented as Paper 87-1545 at the AIAA 22nd Thermophysics Conference, Honolulu, HI, June 8–10, 1987; received Aug. 17, 1987; revision received May 16, 1988.

*Professor of Aeronautical Sciences, Department of Mechanical Engineering. Member AIAA.

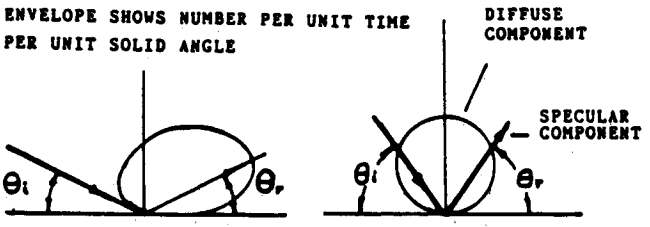

Cell numbers designate axial locations of flowfield profiles.

Cell number	x, Cell center to entrance, mm.	x_1, Cell center to leading edge, mm.
1	0.51	−5.62
9	8.69	2.55
17	16.86	10.75
25	25.58	19.27
33	33.20	27.07
41	41.38	35.25
49	49.55	43.42
57	57.72	51.59

Cell height $y = 0.833$–1.25 mm
Cell length $x = 1.022$ mm
Cell width $z = 20.0$ mm

Fig. 2 Distributions of scattered molecules.

We know from many experiments that the molecular speed distributions of particles scattered from a surface along any ray may be well-represented as a drifting Maxwellian. Nocilla was perhaps the first to recognize this point.[10] The magnitude of the drift velocity U_r and the translational temperature T_r, both directed along that ray, depend on the several physical parameters of the interactions, including the incoming velocity and direction. The question of how to put together a complete description of molecular/surface scattering in a coherent way remains with us. My preference has been to seek such representations from the empirical evidence. However, for interactions at orbital velocities, the quantity of information is extremely small.

For the present work, the models are designated as follows:

1a) Diffuse scattering, energy of the incident molecule fully accommodated to the surface, or

1b) Diffuse scattering, energy partially accommodated to the surface.

2) Specular reflection.

3) A composite involving a fraction f of 1a together with a fraction $1-f$ of 2. Thus, $1-f$ is the fraction of molecules specularly scattered.

4) The Hurlbut-Sherman application of Nocilla's proposal (HSN).[11]

In referring to the "accommodation coefficient," we must differentiate among various possible definitions. The "partial accommodation coefficient," which finds application in these studies, may be written.

$$\alpha \equiv \alpha(\theta_i) = \frac{e_i\,(\theta_i) - e_r}{e_i\,(\theta_i) - e_w} \tag{1}$$

in which $e_i\,(\theta_i)$ is the energy carried to the surface by the incident flow along the angle θ_i as measured from the surface tangent, e_w the mean energy that would be carried from the surface if all particles were scattered in Maxwellian remission, i.e., diffusely, from the wall at temperature T_w, and e_r the mean energy of reflected particles taken over the entire reflected distribution of velocities. In model 1b we understand partial accommodation to imply scattering according to a Maxwellian distribution of velocities at some effective wall temperature not equal to T_w. In standard use, values of α are assumed constant over θ_i.

It should be noted that model 3 or model 1a have almost always been used in DSMC computation. Historically, values of thermal accommodation were customarily obtained through experimentation with thermal conductivity cells. In connection with such measurements, it was frequently asserted that model 3 and model 1b were equivalent descriptions of the scattering process. This conjecture was satisfactory in its time and as appled to static systems. However, as results from molecular beam scattering studies became available, it became clear that pure specular reflection was not observed either by itself or in combination with diffuse scattering. Approximations have been found in classic studies of diffraction maxima, but the conditions for such work are remote from ours. It will be shown in a later section of this paper that model 3 and model 1b lead to quite different flowfields above a flat plate in hypersonic flow.

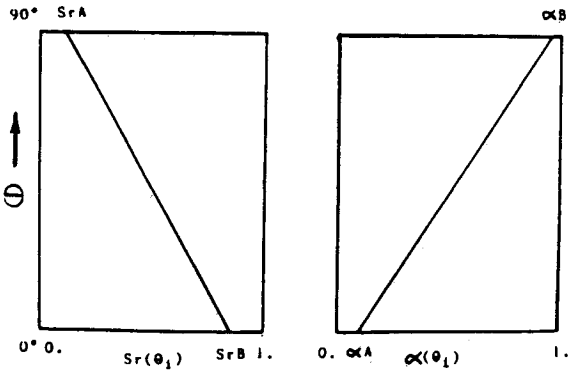

Fig. 3 Functional behavior of $S_r(\theta_i)$ and $\alpha(\theta_i)$.

The Hurlbut-Sherman model[11] coordinates empirical information derived from molecular beam studies in a formulation easily adaptable to computational requirements. The scattered molecular density pattern is, in general, lobular and characterized by the parameters of a drifting Maxwellian. The lobular form is distributed about a central ray that has the velocity U_r and is assumed to take the direction of the reflected ray, i.e., $\theta_i = \theta_r$ (Fig. 2).

The parameters governing the scattering distribution are the reflected molecular speed ratio $Sr(\theta_i)$ and the energy accommodation coefficient $\alpha(\theta_i)$, together with the surface temperature, the properties of the incident flow, and the molecular gas constants. Observed scattering behavior has led me to define, as an idealization, a linear form for the functional description of $Sr(\theta_i)$, which quantity changes from a low value at $\theta_i \approx 90$ deg to a higher value at θ_i near the surface glancing angle. The reverse behavior is observed for $\alpha(\theta_i)$, that is, for small θ_i the energy accommodation is found to be smaller than at $\theta_i \approx 90$ deg. Typical variations of the parameters used in this paper are shown in Fig. 3. It should be clear that more realistic functional forms can be applied when experimental results permit.

It also should be clear that models 1a, 1b, and 2 are contained in 4, at appropriate limits. That is, for $Sr(\theta_i) = 0$, we model diffuse scattering, whereas for $\alpha(\theta_i) = 0$ and $S_r(\theta_i) \gg 10$ we approximate specular reflection. For the cases that generally lie between these limits, model 4 offers the greatest potential for physical representation among those considered here.

Simulations

It would appear that the experimental work most suitable for comparison with the present calculation was conducted at the University of California at Berkeley by Becker et al.[8] during 1973–74. The electron beam/Fabry-Perot fluorescence technique[12,13] was used to measure velocities, densities, and temperatures as functions of location above a flat plate in a hypersonic flow of helium. The Mach number at the leading edge was about 9, the freestream temperature about 10.7 K, and the freestream velocity was 1723 m/s. The freestream mean-free path at the leading edge was calculated to be approximately 1.29 mm.

The length of the wind tunnel model was 50.8 mm. The published data are confined to a field extending from the surface to a distance above it of approximately 5 mm, which unfortunately does not offer comparison above this level with our larger simulation field. Flow conditions of the experimental work have been closely matched in the majority of present simulations, with one possible important difference—a uniform, parallel stream rather than a field having the slight divergence of the free jet flow, has been used here. Note will be taken of this difference in remarks to follow. Helium flows at an entering freestream number density of $0.23 \times 10^{22}/m^3$; freestream velocity of 1723 m/s, and freestream temperature of 10.7 K were used.

Surface scattering parameters were selected to explore increasing departures from model 1a, diffuse scattering with full accommodation, which serves as a baseline model and which was imagined to closely approximate scattering behavior for the tunnel results. The parametric changes consisted first, in small reductions in accommodation coefficient while retaining diffuse scattering, then in specifying a range for α within the format of the HSN model (model 4), then permitting some lobularity within this framework by allowing $Sr(\theta_i)$ to depart from zero. As a final modification, the effects of model 3 were examined using a value of $f = 0.5$. Conditions for the 12 simulations used in this study are shown in Table 1.

Table 1 Simulation conditions

Case	S_rA	S_rB	A	B	Z
1	0.0	0.0	1.0	1.0	0.1446
2	0.0	0.0	0.5	0.9	0.1475
3	0.0	0.0	0.4	0.8	0.1452
4	0.0	0.3	0.4	0.8	0.1318
5	0.1	0.3	0.4	0.8	0.1296
6	0.2	0.5	0.4	0.8	0.1150
7	0.3	0.6	0.4	0.8	0.1105
8	0.3	0.8	0.4	0.8	0.1011
9	0.3	1.0	0.3	0.7	0.0950
10	0.3	1.5	0.3	0.7	0.0817
11	0.0	0.0	1.0	1.0	0.0541[a]
12	0.0	0.0	0.5	0.5	0.1468

[a]Composite model 3; $f = 0.5$.

Results

Characteristic features of results may be seen from the baseline representation in Fig. 4. These show velocity, temper-

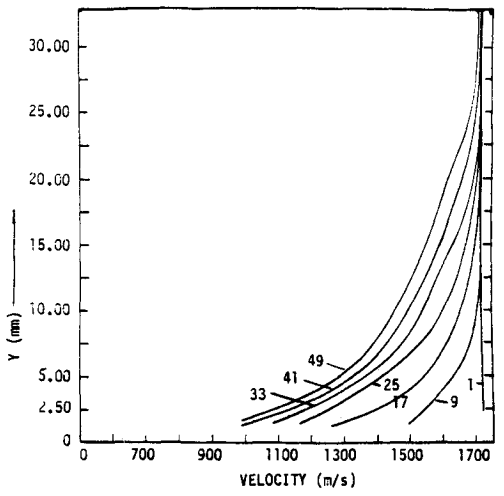

a) Gas velocity vs distance Y above surface

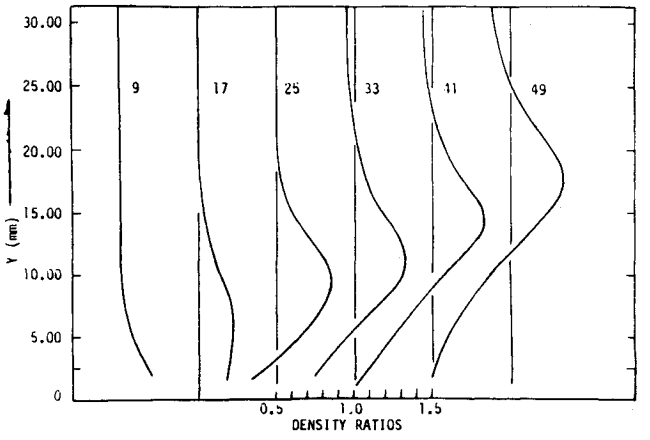

c) Ratio of local gas density to initial freestream density

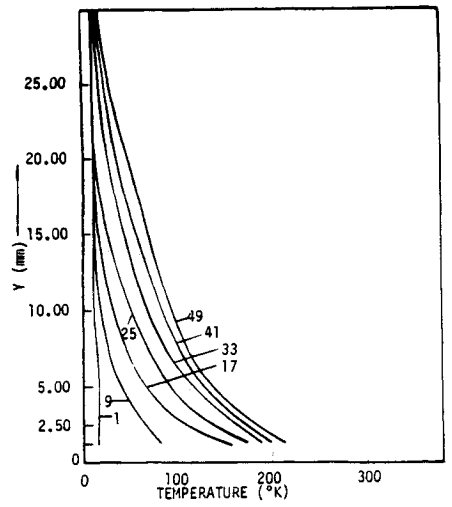

b) Gas temperature vs distance Y above surface

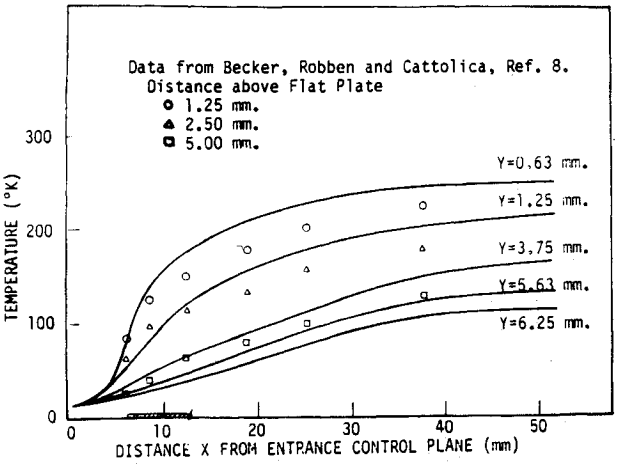

d) Axial dependence of gas temperature

Fig. 4 Baseline distributions—full thermal accommodation with diffuse scattering.

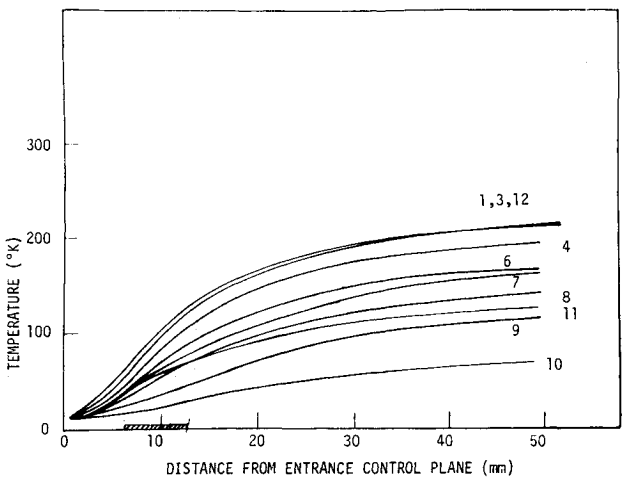

Fig. 5 Axial dependence of gas temperature at 1.25 mm above surface. Curves are identified by case numbers. See Table 1.

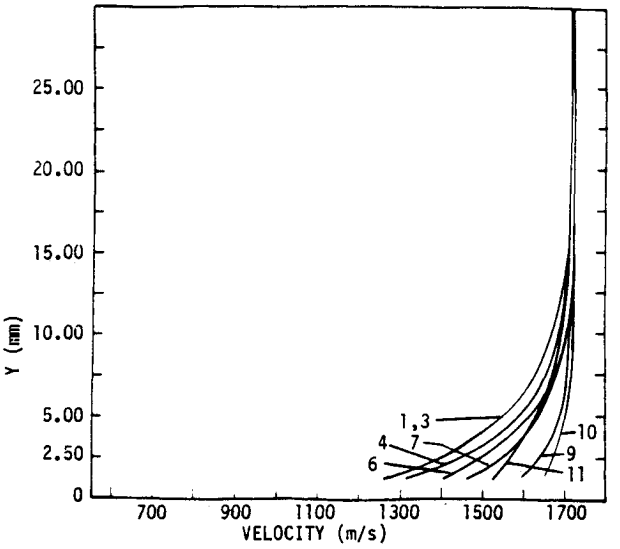

a) Velocity vs distance above surface at $X_1 = 10.75$ mm

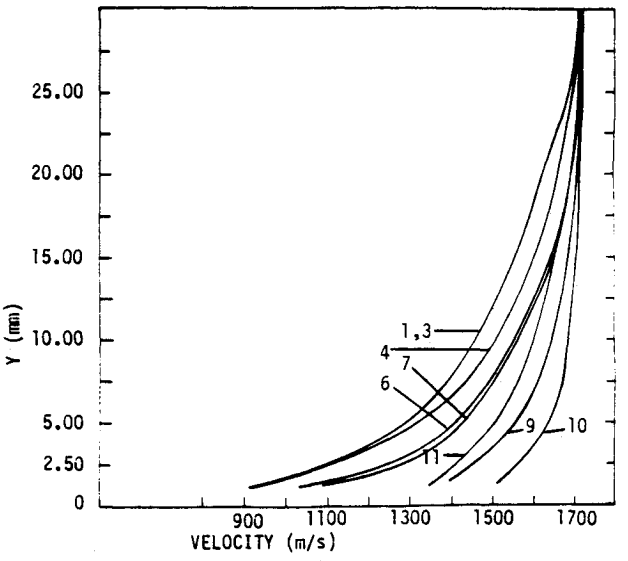

b) Velocity vs distance above surface at $X_1 = 43.42$ mm

Fig. 6 Comparison of velocity profiles. Curves are designated by case numbers. See Table 1.

ature, and density profiles at axial locations defined in Fig. 1. One immediately sees the strong temperature jump and velocity slip near the leading edge. Both are seen to diminish rapidly as the axial location is increased. In Fig. 4c, one sees the well-marked density bulge and run-out toward and away from the surface marking the fully merged shock. The shock wave can also be seen in the velocity profile for station 49, Fig. 4a, as a sudden decrease in velocity as one follows the curve from the top towards the surface.

The dependence of temperature on axial location at five values of the Y coordinate, shown in Fig. 4d, provides an excellent opportunity for comparison of DSMC results with those of Becker et al.[8] Quite good quantitative agreement is seen although in no case would we claim really close correspondence. For example, the measured value at $Y = 1.25$ mm and $X = 38$ mm lies at a temperature about 10% larger than the calculated value. The measured quantities are for the most part correctly bracketed by the calculated values, and the forms of the respective distributions are satisfactorily similar.

Examination of the temperature change is continued (Fig. 5), in which axial distributions are plotted for 10 cases, including the baseline case. In one sequence, all with the same range in α, i.e., $\alpha A = 0.4$, $\alpha B = 0.8$, each incremental increase in lobularity effected through a change in the range or magnitude of $Sr(\theta_i)$ (see Table 1) brings about a decrease in the magnitude of the temperature function. The "family" is not as well ordered as one would like; certain variations of slope and form demand further exploration.

In each simulation, the total number of helium atoms, Nout, leaving the downstream control surface was recorded, as was the number of atoms striking the active surface, NW1. One may define a quantity Z such that

$$Z = \text{NW1/Nout} \tag{2}$$

The ratio Z was conjectured to be an integrated measure of the "impedence" offered the flow by the active surface. The word "impedence" is used very loosely, since both thermal energy and momentum transfers at the surface effect subsequent flow interactions. Values of this ratio for the several cases are shown in Table 1, along with the associated scattering parameters.

The relationship between the order of Z and the values of the scattering parameters is intuitively plausible, except for the order of the first three. While these values of Z are very close together, one would expect Z to be the largest for the baseline condition. One may suggest that smaller thermal accommodation leaves the diffusely scattered molecules with smaller scattered velocities and, hence, with a greater probability of scattering with the incoming stream close to the surface. A relatively larger number of surface encounters will result.

From Fig. 5, one sees that a small amount of lobular scattering, as in case 4, produces a significant change in the axial distribution of temperature, a change which is also reflected in the value of Z. The temperature of the field is substantially reduced with each additional increase in lobularity.

When the value of the thermal accommodation coefficient is held constant at $\alpha A = \alpha B = 0.5$, as in case 12, the resultant value of Z is 0.144, very close to case 2. In this instance we have computed for model 1b as a special case of model 4. We see that this result is far removed from that of model 3, with $f = 0.5$, for which the value of Z is only 0.054. With the introduction of true specularity, we make a profound change in the flowfield. It should be clear that the two interpretations of accommodation coefficient are quite dissimilar.

The axial distance over which changes in flowfield structure and reductions in the number of surface encounters will be significant is not shown by our limited simulation. The effects near the leading edge on heat transfer and, presumably, on chemical reactions may well be quite large.

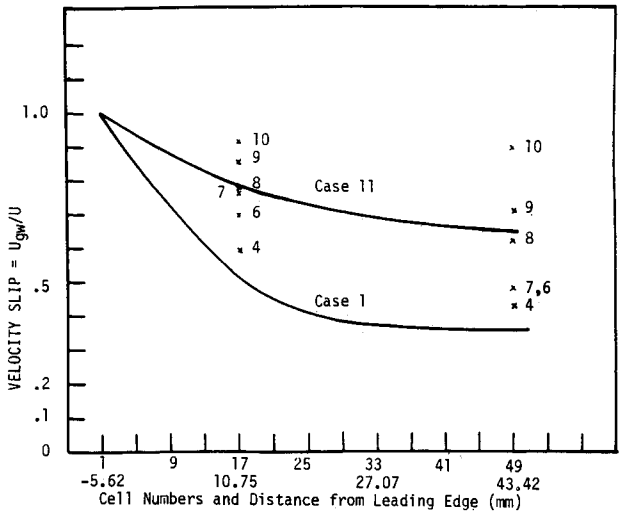

Fig. 7 Velocity slip. Numbers on plot refer to cases. See Table 1.

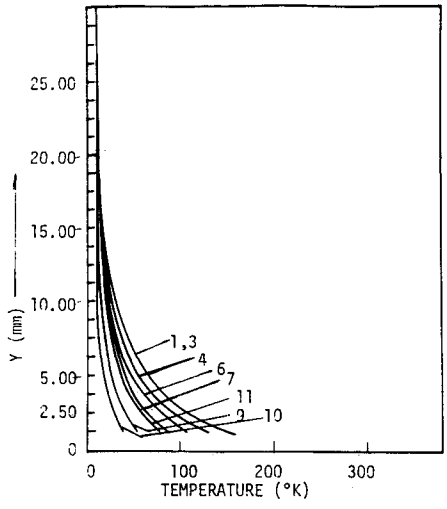

a) Temperature vs distance above surface at $X_1 = 10.75$ mm

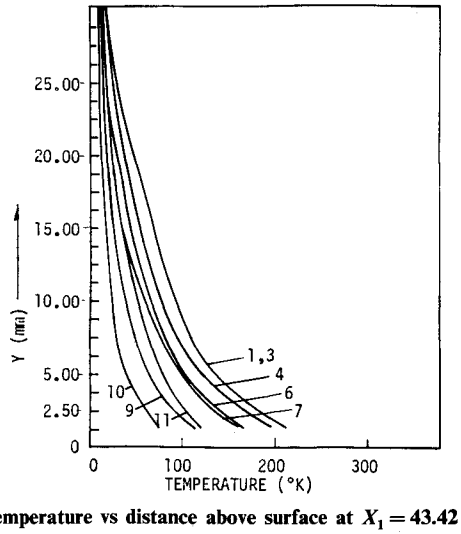

b) Temperature vs distance above surface at $X_1 = 43.42$ mm

Fig. 8 Comparison of temperature profiles. Curves are designated by case numbers. See Table 1.

Velocity profiles from the several simulations are shown in Fig. 6a at an axial location 10.75 mm downstream from the leading edge, and in Fig. 6b at 43.42 mm. Figure 6b is particularly useful in showing the remarkable increase in velocity near the wall and for a distance of several mean free paths above the surface, as greater lobularity and smaller thermal accommodation are introduced. This progression in

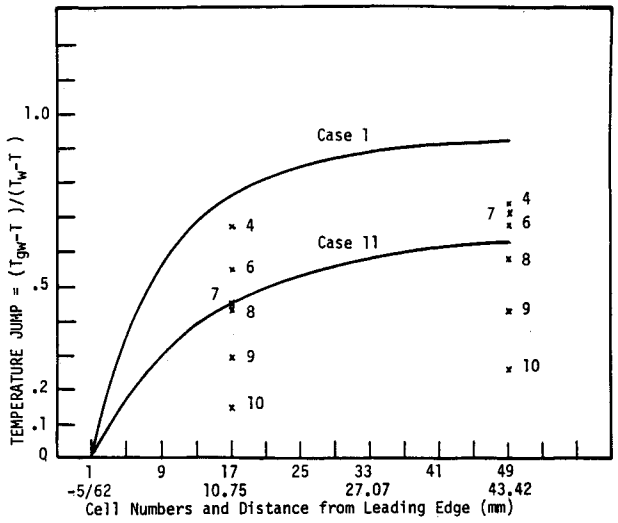

Fig. 9 Temperature jump. Numbers on plot refer to cases. See Table 1.

velocity patterns follows the progression toward lower values of Z. Velocity slip for the two cases is plotted in Fig. 7. These follow trends that are consistent with the foregoing observations.

In analogous fashion, temperature profiles from the several simulations are shown in Fig. 8a for $x_1 = 10.75$ mm, and $x_1 = 43.42$ mm in Fig. 8b. Nesting of these curves also follows the progression toward lower Z. Temperature jump for the two stations are plotted in Fig. 9. Temperature and velocity profiles do not form an exact mirror image set, but the similarities are strong.

The ratio R of local gas density to entering freestream density was introduced in Fig. 4c, wherein are shown plots of this ratio for the baseline case as a function of y at six axial stations. In Fig. 10, R is shown for several cases at axial locations $x_1 = 27.07$ mm and at $x_1 = 43.42$ mm, as measured downstream from the leading edge. It is interesting to observe that the largest change in density ratio from the surface value to a maximum in the shock center occurs for the baseline case. It is also apparent that these ratios show increasingly smaller changes with greater lobularity. On the other hand, density ratio profiles computed using model 3 (case 11), with $f = 0.5$, show the influence of the fraction, which is diffusely scattered. Profiles of case 11 should be compared with case 10, which shows a flatter pattern but yields a larger value of Z.

Summary

Studies of rarefied hypersonic flow of helium over a flat plate in which the method of DSMC was used to provide detailed descriptions of velocity, temperature, and density throughout the simulated field are described. There are two focii of attention: 1) to examine the effects of various surface interaction models with appropriate parametric variations, and 2) to compare the results of simulations with flowfield data resulting from laboratory experiment.

It can be said immediately that agreement of simulation results with the experimental flowfield was remarkably close near the leading edge but became less exact downstream.

It was found that surface interaction models providing departures from diffuse scattering toward increasing lobularity resulted in diminishing values of the ratio between molecule wall encounters and molecules emerging through the downstream control surface. There were corresponding striking changes in velocity, temperature, and density profiles. There is much reason to believe, based upon experiment, analysis, and simulation[1,9] that scattering at the vehicle surface will exhibit lobularity. Computation predicting flow dynamics and chemistry must incorporate correct representations of the surface interactions and these must come from a renewed experimental effort.

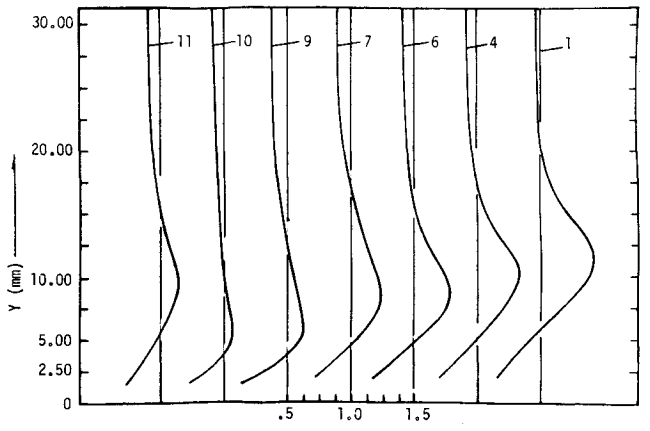

a) $X_1 = 27.07$ mm

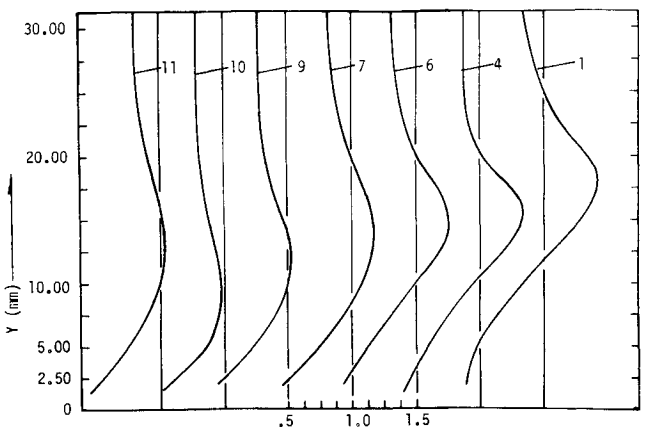

b) $X_1 = 43.42$ mm

Fig. 10 Density ratio vs distance Y above surface. Curves are designated by case numbers. See Table 1. Profiles calculated at distance X_1 downstream from leading edge.

References

[1]Moss, J. N. and Bird, G. A., "Direct Simulation of Transitional Flow for Hypersonic Re-entry Conditions," *Progress in Astronautics and Aeronautics: Thermal Design of Aeroassisted Orbital Transfer Vehicles*, edited by H. F. Nelson, Vol. 96, AIAA, New York, 1985, pp. 113–139.

[2]Moss, J. M., "Direct Simulation of Hypersonic Transitional Flow," *Proceedings of the 15th International Symposium on Rarefied Gas Dynamics*, edited by V. Boffi and C. Cercignani, B. G. Teubner, Stuttgart, FRG, 1986, pp. 384–399.

[3]Cuda, V. and Moss. J. N., "Direct Simulation of Hypersonic Flows, Over Blunt Slender Bodies," AIAA Paper 86-1348, June 1986.

[4]Bird, G. A., *Molecular Gas Dynamics*, Clarendon Press, Oxford, England, UK, 1976.

[5]Dahlen, G. A. and Brundin, C. L., "Wall Temperature Effect on Hypersonic Cone Drag," *Proceedings of the 13th International Symposium on Rarefied Gas Dynamics*, Novosibirsk, USSR, 1982, edited by O. M. Belotserkovskii et al., Vol. 1, Plenum Press, 1985, pp. 453–460.

[6]Bird, G. A., "Rarefied Hypersonic Flow Past a Slender Sharp Cone," *Proceedings of the 13th International Symposium on Rarefied Gas Dynamics*, Novosibirsk, USSR, 1982, edited by O. M. Belotserkovskii et al., Vol. 1, Plenum Press, 1985, pp. 349–356.

[7]Hurlbut, F. C., "Rarefied Hypersonic Flow Over a Flat Plate Using DSMC," 15th International Symposium on Rarefied Gas Dynamics, Grado, Italy, 1986.

[8]Becker, M., Robben, F., and Cattolica, R., "Velocity Distribution Function Near the Leading Edge of a Flat Plate," *AIAA Journal*, Vol. 12, 1974, p. 1247.

[9]Hurlbut, F. C., "Gas Surface Scattering Models for Satellite Applications," *Progress in Astronautics and Aeronautics: Thermophysics Aspects of Re-Entry Flows*, edited by J. M. Moss and C. D. Scott, Vol. 103, AIAA, New York, 1986, pp. 97–119.

[10]Nocilla, S., "On the Interaction Between Stream and Body in Free-Molecule Flow," *Advances in Applied Mechanics, I: Rarefied Gas Dynamics*, edited by L. Talbot, Academic, New York, 1961, pp. 169–208.

[11]Hurlbut, F. C. and Sherman, F. S., "Application of the Nocilla Wall Reflection Model to Free-Molecule Kinetic Theory," *Physics of Fluids*, Vol. 11, March 1968, pp. 486–496.

[12]Cattolica, R. J., "An Experimental Study of Transitional Nonequilibrium in Free Jet Expansion," College of Engineering, Univ. of California, Berkeley, Rept. FM 72-6, Dec. 1972.

[13]Cattolica, R. J., Robben, F., and Talbot, L., "The Ellipsoidal Distribution Function and Transitional Equillibrium," *Proceedings of the 9th International Symposium on Rarefied Gas Dynamics*, edited by M. Becker and M. Fiebig, Vol. 1, DFVLR Press, Portz-Wahn, FRG, pp. B16-1–B16-11, 1974.